Clays and Clay Minerals, Vol. 32, No. 5, 375–383, 1984.

NONTRONITE IN A DEEP-SEA CORE FROM THE SOUTH PACIFIC

A. SINGER,[1] P. STOFFERS,[2] L. HELLER-KALLAI,[1] AND D. SZAFRANEK[1]

[1] Hebrew University of Jerusalem, Rehovot, Israel

[2] Institut für Sedimentsforschung, Universität Heidelberg, Heidelberg, Germany

Abstract—Smectite close to the pure Fe end member of the nontronite-beidellite series was found in the fine clay separated from a 354-cm deep sediment core in the southwestern Pacific Basin. The mineral has a *b*-axis of 9.09 Å and an unusually low dehydroxylation temperature of 454°C and is composed of sheaves of fibers less than 50 Å wide. Its charge density is 5.09×10^{-4} esu/cm^2. The charge originates mainly from the presence of 18% of the total Fe in tetrahedral positions, as determined by Mössbauer analysis. Slight deviations of the infrared spectra from those reported for nontronites are probably due to the presence of more octahedral Mg. The presence of authigenic quartz in the same sample permits some speculation on the concentration of dissolved silicon during nontronite genesis. A $\delta^{18}O$ value of $26 \pm 0.3‰$ indicates a temperature of formation of about 22°C. The Sr isotope ratio suggests that the nontronite formed at least 12 million years ago.

Key Words—Age, Charge density, Deep sea, Iron, Mössbauer spectroscopy, Nontronite, Oxygen isotopes.

INTRODUCTION

Nontronite and beidellite form a continuous solid solution, but, although the pure iron end member has been predicted, the chemical composition of all specimens described until recently includes at least small amounts of Al (Weaver and Pollard, 1973; Eggleton, 1977). Marine clays of hydrothermal origin, however, have been reported to approach the pure Fe end member (Corliss *et al.*, 1978; Hoffert *et al.*, 1978; Schrader *et al.*, 1980; Moorby and Cronaw, 1983; McMurtry *et al.*, 1983).

Clay material recovered during the 1980 cruise SO-14 R.V. of "Sonne" in the southwestern Pacific Basin has been found to contain some layers that consist of nearly pure nontronite containing only a trace amount of Al. The present paper describes the physical and chemical properties of this material and speculates on its origin.

MATERIALS AND METHODS

Core description

As part of an extensive survey of manganese nodule distribution in the southwestern Pacific Basin, a drill core (KL9) was recovered on the transect Tahiti-East Pacific Rise-New Zealand at 29°28.08'S, 131°36.81'W in 4250 m water depth. The drill hole was located on the western flank of a small seamount ranging from 4260 to 3990 m depth in a north to south striking valley. The structural setting of the sampling area is unknown because no detailed geophysical survey was carried out. The core is 354 cm long. The upper 190 cm of the core consists of a dark brown, homogeneous, fine-grained material. Rather abruptly, at 189 cm depth, the material changes to an aggregate of coarse-sand size, greenish yellow to orange granules, some of which are partly coated by Mn oxides. The Mn oxide coatings increase in abundance with increasing core depth, and at 210 cm core depth the coating envelopes are essentially complete. Mn oxides cement the granules into larger aggregates, thereby creating dark gray layers; the most conspicuous one is at 210–215 cm core depth. The Mn oxides consist of todorokite and birnessite. Below 215 cm Mn oxides are less abundant and disappear almost entirely near 300 cm. At 302–310 cm only slight coatings are present. The amount of Mn oxide coatings appears to decrease with increasing grain size. Uncoated granules are light yellowish green. From scanning electron micrographs and X-ray powder diffraction patterns the granules consist of typical smectite aggregates, coated by birnessite. Numerous quartz crystals are embedded in the clay matrix or coat the clay granules and can be discerned by their glitter.

Sample treatment

Preliminary examinations indicated that the smectite was best developed in the lower parts of the core. Therefore, nodule material from 230–260 cm, 340–355 cm, and from the core catcher (the lowest part of the core) was examined in detail. The samples were washed in distilled water and dispersed ultrasonically. They were then rewashed in 1 N NaCl, and the excess salt was removed. The Na-saturated and dispersed samples were then resuspended in distilled water, and the fine clay (<0.6 μm) fractions were separated by sedimentation. Untreated granules were also examined by X-ray powder diffraction (XRD).

Analyses

XRD analyses were made with a Philips diffractometer using CuKα radiation. Differential thermal analysis was performed on a Perkin-Elmer high-tempera-

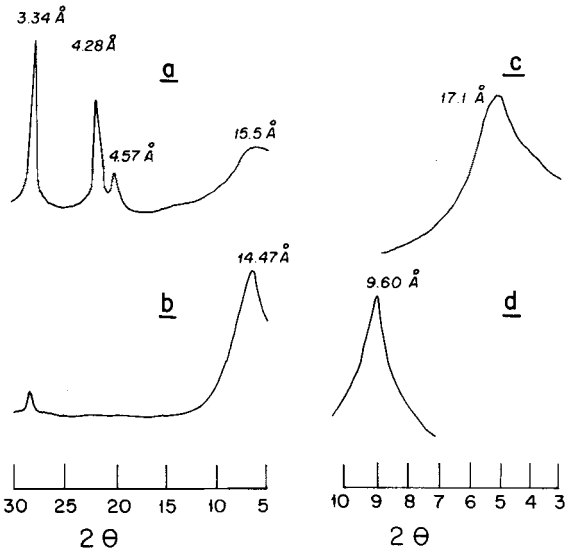

Figure 1. X-ray powder diffraction patterns of material from core KL9; (a) untreated bulk material from an uncoated nodule at 230–260-cm depth; (b) untreated oriented clay (<2 μm) separated from the nodule; (c) glycolated clay; (d) clay heated to 500°C. (CuKα radiation.)

ture 1700 DTA at a heating rate of 10°C/min. Transmission electron microscopy (TEM) was carried out with a JEM 100CX instrument. For selective area electron diffraction (SAD), gold was used as internal

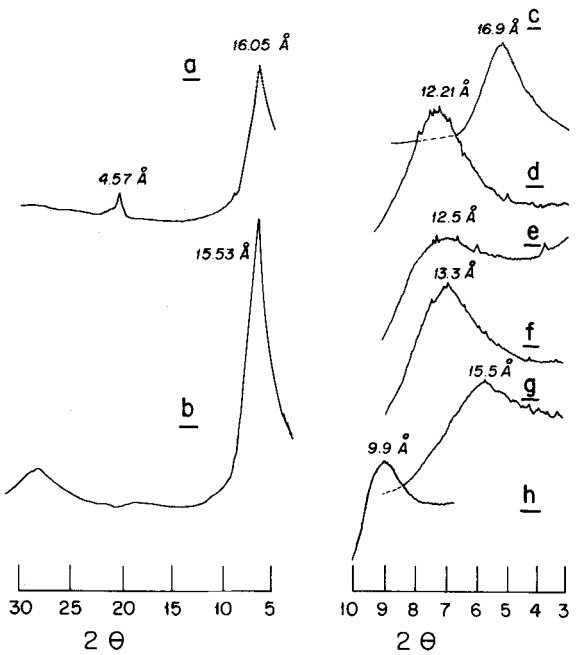

Figure 2. X-ray powder diffraction patterns of fine (<0.6 μm) clay separated from layer at 340–355 cm depth; (a) Mg-saturated, unoriented; (b) oriented; (c) glycolated; (d) air-dried, K-saturated; (e) air-dried, NH_4^+-saturated; (f) K-saturated, glycolated; (g) NH_4^+-saturated, glycolated; (h) Mg-saturated, heated to 250°C for 2 hr. (CuKα radiation.)

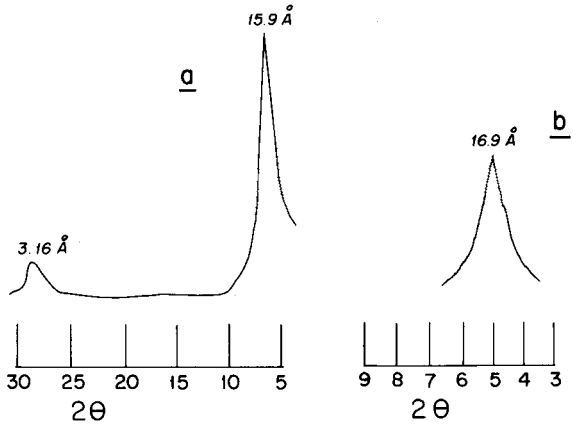

Figure 3. X-ray powder diffraction patterns of fine (<0.6 μm) clay separated from the core catcher; (a) Mg-saturated, oriented; (b) Mg-saturated, glycolated.

standard. Infrared (IR) spectra were obtained from samples prepared in the form of KBr disks and as self-supporting films, using a Perkin-Elmer 237 spectrometer to record the spectra in the 4000–650-cm^{-1} range. For Mössbauer spectroscopy, 9 mg of sample (equivalent to 2.2 mg Fe) mixed with glucose was placed in a Lucite holder 1 cm in diameter and examined by the procedure described by Rozenson *et al.* (1979).

The chemical composition was determined by X-ray fluorescence analysis, using a Philips PW 1400 X-ray spectrometer with an one-line Philips PH 851 computer. Atomic absorption spectroscopy was used to determine Al, Co, and Ca after the samples were decomposed with lithium meta-borate. The cation-exchange capacity (CEC) was determined by sodium saturation; specific surface area (SSA) was determined using ethylene glycol monoethyl ether (Carter *et al.*, 1965). $\delta^{18}O$ and $^{87}SR/^{86}Sr$ values were determined using standard techniques. Free iron oxides were removed by sodium dithionite treatment.

RESULTS AND DISCUSSION

X-ray powder diffraction analysis

XRD patterns of powdered bulk material from the 230–260-cm layer gave distinct reflections at 15.5 and 4.57 Å, suggesting the presence of a 2:1 clay mineral saturated with divalent cations (Figure 1). Strong reflections of quartz were also present. The distinct 060 reflection at 1.513 Å indicated the dioctahedral nature of the clay mineral. Untreated and oriented clay material, separated by sedimentation from the granules, gave a strong reflection at 14.47 Å, with a very weak 005 reflection at 3.24 Å, and a faint quartz reflection. Upon glycolation, swelling to 17.1 Å was complete, whereas heating the sample to 500°C for 2 hr shifted the 001 spacing to 9.8 Å.

Unoriented samples of fine (<0.6 μm), Mg^{2+}-satu-

https://doi.org/10.1346/CCMN.1984.0320505 Published online by Cambridge University Press

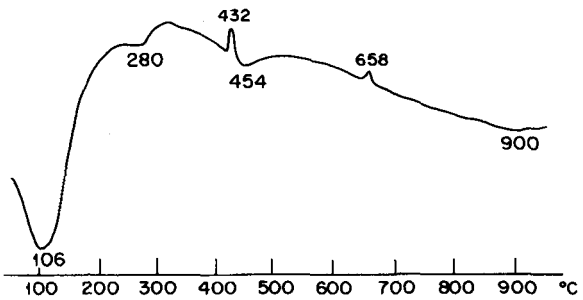

Figure 4. Differential thermal analysis tracings of fine (<0.6 μm) clay separated from the core catcher; exotherms at 432 and 658°C are Ag_2SO_4 calibration peaks.

rated clay separated from the 340–355-cm layer and from the core catcher sample gave a strong basal reflection at 16.05 Å (Figures 2 and 3). No accessory minerals were identified. A 060 reflection at 1.515 Å indicated the dioctahedral nature of the mineral. Oriented samples gave very strong basal reflections at 15.53 Å and very weak 005 reflections. Glycolation resulted in full expansion to 16.9 Å.

Saturation with K^+ at room humidity (50–60% RH) shifted the 001 spacing to 12.2 Å, whereas saturation with NH_4^+ resulted in a diffuse reflection at 12.5 Å. Upon glycolation the K^+-saturated sample expanded to 13.3 Å, and the NH_4^+-saturated sample expanded to 15.5 Å. Thus, with both K^+ and NH_4^+ saturation most of the smectite layers had one interlayer of water molecules. When exposed to ethylene glycol (EG) vapor most of the K^+-saturated smectite layers became interlayered with one EG molecular layer. The basal spacings of the sample saturated with NH_4^+ indicated a 1:1 ratio between smectite layers interlayered with one and those interlayered with two EG layers (Čičel and Machajdik, 1981), suggesting that the smectite is composed of at least two different structural layers. Irreversible collapse of Mg-saturated samples to 10.0 Å was obtained after they were heated to 250°C (Figure 2). K^+- and NH_4^+-saturated samples, after being heated at this temperature, still had a spacing of 10.6 Å. Final collapse to 10.0 Å occurred only after the samples had been heated to 300°C. Apparently, irreversible collapse was obtained only after the removal of the water, which gave rise to an endotherm at about 280°C on the DTA curve (see below).

From repeated determinations of the 060 spacing, the *b*-axis of the nontronite is equal to 9.08 Å for the granular material collected at 230–260 cm depth and 9.09 Å for the nontronite collected at 340–355 cm depth. These values are close to those expected from the relationship between the length of the *b*-axis and the number of Fe^{3+} ions per unit-cell as given by MacEwan (1961) and Brigatti (1983), but are lower than those based on (Fe + Mg) in the equation proposed by Despraires (1983).

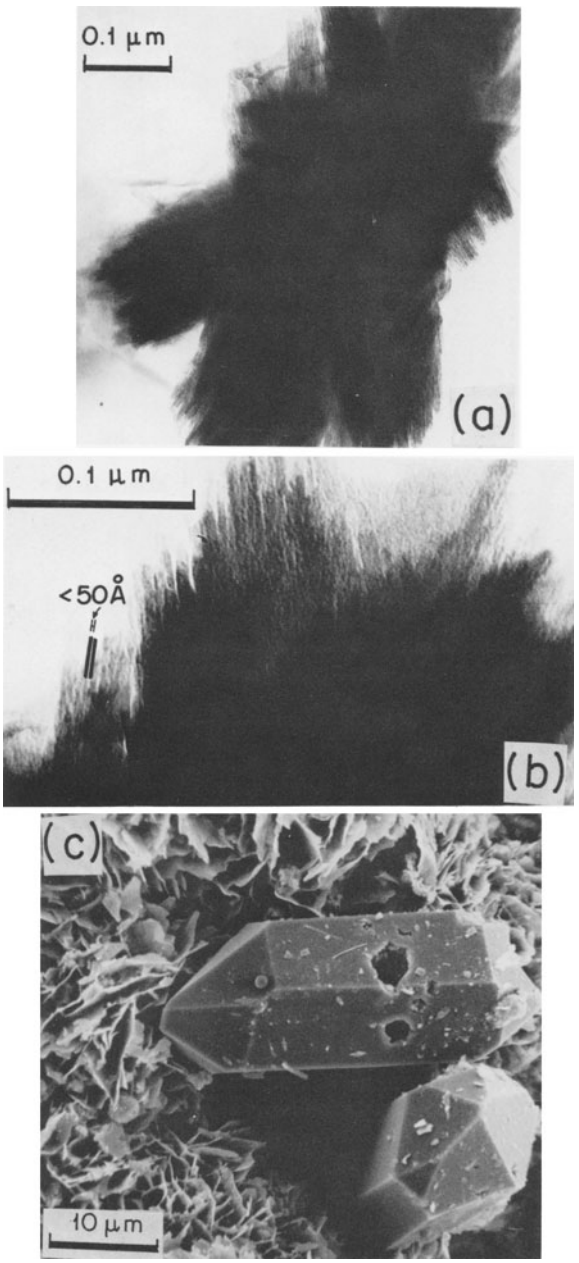

Figure 5. (a), (b) Transmission electron micrographs of fine clay separated from layer at 340–355 cm depth; (c) authigenic quartz embedded in nontronite clay matrix, from layer at 200–205 cm depth.

Differential thermal analysis

The differential thermal analysis curve of Mg-saturated material, equilibrated at room humidity (50–60% RH), shows a very strong endotherm at 106°C, followed by a very weak endotherm at 280°C (Figure 4). These endotherms are associated with the loss of adsorbed water and cation hydration water, respectively. The dehydroxylation endotherm at 454°C fits the cor-

https://doi.org/10.1346/CCMN.1984.0320505 Published online by Cambridge University Press

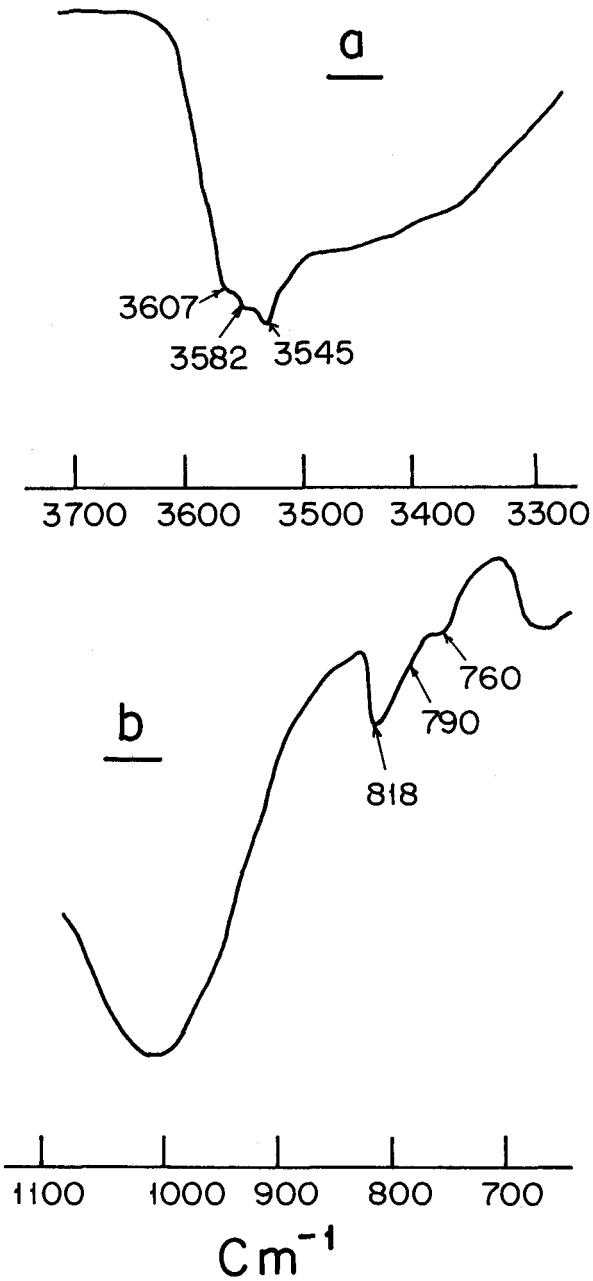

Figure 6. Infrared spectrum of NH_4-saturated fine clay from layer at 340–355 cm depth; (a) 3700–3300-cm^{-1} region, self-supporting film; (b) 1100–650-cm^{-1} region, KBr disk.

relation curve between dehydroxylation peak temperature vs. *b* dimension, and, by implication, Fe content, established by Brigatti (1983). The curve is similar to that given by Rateev *et al.* (1980) for K-, Fe-smectites from the Galapagos geothermal field.

Electron microscopy

Transmission electron micrographs of finely dispersed samples show elongated, feathery flakes (Figure 5). Moderately dispersed samples showed "mossy" aggregates, similar to the Cheto-type smectites described by Grim and Güven (1978) from Arizona. Under high magnification these aggregates appeared to be composed of very thin fibers, less than 50 Å wide, arranged parallel in bundles, which in turn are oriented at various angles to each other, forming sheaves (Figures 5a and 5b). Whether these fibrous units, which appear to represent primary particles, formed by curling of thin layers or ribbons is difficult to establish. Nontronites generally occur in the form of laths or ribbons. Nontronite from Pfaffenreuth, Bavaria (Méring and Oberlin, 1971) is lath shaped, with free particles of a mean width of ~2000 Å and has a strong tendency for end-to-end association, yielding long ribbons. Sudo *et al.* (1981) described Fe-montmorillonite with lath-like, platy particles without well-defined borders, with some particles having a feather-like appearance. Cole and Shaw (1983) and Kurnosov *et al.* (1982) described fibrous nontronites, but the fibers were much coarser than those of the KL9 clay. Grim and Güven (1978) showed trioctahedral Mg-smectites from the Amargosa Valley, Nevada, that exhibit sheaf-like aggregates of fibers.

Mössbauer spectroscopy

The experimental Mössbauer spectrum could be well fitted by three doublets, two corresponding to Fe^{3+} in octahedral and one to Fe^{3+} in tetrahedral coordination. The parameters obtained by least squares computer fit are as follows:

Octahedral								Tetrahedral			
IS	QS	Γ	%	IS	QS	Γ	%	IS	QS	Γ	%
0.42	0.68	0.43	25	0.37	0.27	0.41	57	0.22	0.65	0.34	18
±0.01	±0.02	±0.04	±7	±0.01	±0.02	±0.04	–	±0.01	±0.03	±0.05	±5

where IS = isomer shift relative to metallic Fe; QS = quadrupole splitting; Γ = peak width; all in mm/sec.

These parameters closely resemble those reported for nontronites by Goodman *et al.* (1976), indicating that the relatively high concentration of Mg in this sample does not significantly affect the configuration of the octahedral sheets.

Infrared spectra

Si–O stretching absorption. An intense Si–O stretching absorption was noted at 1005 cm^{-1} (Figure 6b), in complete agreement with the results of Goodman *et al.* (1976), who correlated the position of this band in nontronites with the amount of Fe^{3+} in tetrahedral sites. The percentage of total iron occupying tetrahedral positions in sample KL9 is 17% by chemical analysis and 18% by Mössbauer spectroscopy. Goodman *et al.* observed a frequency of 1006 cm^{-1} for samples with 19–27% tetrahedral Fe^{3+}.

Table 1. Chemical composition of KL9 nontronite from the South Pacific and other hydrothermal nontronites.

	1	2	3	4	5	6	7	8	9	10	11
						wt. %					
SiO_2	45.5	36.4	38.83	47.12	44.68	44.06	38.42	29.1	40.24	41.86	50.39
Al_2O_3	0.2	0.4	0.2	0.34	0.89	0.47	1.05	1.92	4.26	4.29	0.027
Fe_2O_3	37.9	38.6	34.33	31.75	29.13	25.51	21.59	36.96	26.68	27.45	36.24
MnO	1.07	3.78	4.72	0.129	0.1	0.092	3.52	0.84	0.75	0.6	0.09
MgO	2.91	2.73	2.77	3.018	3.27	3.42	3.25	1.17	2.94	2.84	3.75
CaO	0.6	2.9	1.63	0.68	0.34	1.23	1.21	5	0.67	0.66	n.d.
Na_2O	1.71	1.70	1.89	1.67	1.89	1.88	1.89	0.75	3.09	—	0.03
K_2O	3.23	2.77	3.05	3.83	2.94	2.73	1.89	0.72	2.4	2.33	1.68
TiO_2	0.02	0.02	0.02	0.02	0.02	0.027	0.045	7	0.19	0.2	0.01
Icn	6.22	9.53	8	7.745	16.6	13.72	16.93	20.87	18.45	15.21	7.70
Si/Al	34.45	9.93	172.57	122.1	44.3	85.6	32.6	13.44	8.34	8.60	—
Fe/Mn	152.79	61.11	6.58	246.8	291.28	251.4	5.55	39.8	32.2	41.80	—
P_2O_5	—	—	—	—	—	—	—	—	—	—	0.04
						ppm					
Co	2	8	4	4	—	6.6	5.6	—	56	59	10
Cu	46	55	59	—	—	70.5	91	6100	50	50	n.d.
Ni	2	116	27	3	—	27	52	—	119	88	6
Zn	6	36	6.6	2	—	106	127	25,700	—	365	107
Cd	—	—	—	—	—	13	2	—	—	—	—
Sn	59	300	198	43	—	130	138	—	—	—	—
Ba	43	63	76	74	—	507	773	—	—	—	33
V	5	270	35	—	—	32	40.4	—	107.6	97	82
Cr	4	8	10	—	—	13.5	12.6	—	35	33	28
B	75	529	566	—	—	359	295	—	—	—	—
Ca	2	5	5	—	—	2.5	17	—	—	—	—
Pb	—	—	—	—	—	74	263	—	—	11	3
Rb	—	—	—	—	—	—	—	—	—	—	47
Sr	—	—	—	—	—	—	—	—	—	—	38[1]
Fe_2O_3	(DCB extractable)			—	—	—	—	—	—	—	0.09%

Samples 1–10 = hydrothermal nontronites: samples 1–3 (FAMOUS); 4–5 (Aden); 6–7 (Galapagos); 8 (Red Sea); 9–10 (Cyamex); compilation after Hoffert (1980). Sample 11 = South Pacific, KL9, core catcher (<0.6 μm). n.d. = not detected.
[1] Separation of Sr for $^{87}Sr/^{86}Sr$ analysis showed that this value is too high and that the concentration of Sr is about 8 ppm.

OH-stretching and -bending absorptions. A main OH-stretching absorption band was noted at 3545 cm^{-1}, with shoulders at 3582 and 3607 cm^{-1} (Figure 6a). Changes due to orientation of the film were difficult to observe. As Fe–OH–Fe is the predominant grouping in the octahedral sheets, the band at 3545 cm^{-1} must be due to OH-stretching vibrations for this grouping. The band, which was also observed in spectra of the KBr discs, was noted at a lower frequency in sample KL9 than in any of the samples studied by Goodman *et al.* (1976), probably due to the considerably higher Mg content of sample KL9. The shoulders at 3582 cm^{-1} must then be due to Fe–OH–Mg and Mg–OH–Mg associations, respectively; however, if the distribution of cations in the octahedral sheet is random, the Mg–OH–Mg absorption should have been very weak. The fact that a pronounced shoulder was recorded suggests that some clustering of Mg ions must be present in the octahedral sheets.

Similar considerations apply to the OH-bending vibrations (Figure 6b). Following Goodman *et al.* (1976), the absorption at 818 cm^{-1} may be assigned to Fe–OH–Fe and the inflection at about 790 cm^{-1} to FE–OH–Mg vibrations. If these assignments are correct, the intensity of this absorption supports the suggestion that the incidence of Mg–OH–Mg groups is greater than would be expected from a random distribution of octahedral cations. The absorptions at 3607 and 760 cm^{-1} have not previoulsy been reported for nontronites, because all of the samples studied had much lower Mg contents. A shoulder at about 760 cm^{-1} was detected in some of the spectra of K-, Fe-smectites by Rateev *et al.* (1980), but was not discussed by them.

Chemical composition

The chemical analysis of the fine clay from the core catcher shows an extremely low Al content for this nontronite (Table 1, column 11). Marine hydrothermal nontronites commonly are low in Al (Table 2). Similar low Al contents were reported by Corliss *et al.* (1978) and more recently by McMurtry *et al.* (1983) for nontronite from the Galapagos hydrothermal mound. The Fe content of the clay from core KL9 is high. The free (dithionite-extractable) iron content is only 0.09%, and no crystalline iron oxides were identified, indicating that nearly all of the iron is within the clay mineral.

Table 2. Structural distribution of cations in hydrothermal nontronites and the KL9 nontronite.[1]

FAMOUS (Cyp 74.26.151a)	$(Ca_{0.01}Na_{0.51}K_{0.64})(Fe^{3+}_{3.49}Mg_{0.67})(Si_{7.02}Al_{0.03}Fe^{3+}_{0.94})$
Aden (6243-12)	$(Ca_{0.13}Na_{0.57}K_{0.68})(Fe^{3+}_{3.14}Mg_{0.79})(Si_{7.4}Al_{0.17}Fe^{3+}_{0.42})$
Galapagos (424-2-4-30-33)	$(Ca_{0.03}Na_{0.45}K_{0.75})(Fe^{3+}_{3.12}Mg_{0.91})(Si_{7.56}Al_{0.06}Fe^{3+}_{0.38})$
Red Sea (120 K)	$(Ca_{2.07}Na_{0.45}K_{0.712})(Fe^{3+}_{1.27}Fe^{2+}_{1.71}Mg_{0.77})(Si_{5.86}Al_{0.35}Fe^{3+}_{1.79})$
Cyamex (Cyp 78 07 13)	$(Ca_{0.09}Na_{0.12}K_{0.65})(Fe^{3+}_{3.47}Mg_{0.66})(Si_{7.28}Al_{0.08}Fe^{3+}_{0.64})$
KL 9 (core catcher, <0.6 μm)	$((NH_4)_{0.69}K_{0.30})(Fe^{3+}_{3.32}Mg_{0.81})(Si_{7.33}Fe^{3+}_{0.67})$

[1] Compilation of data after Hoffert (1980).

Similar Fe contents were also reported by Bischoff (1972) for a ferroan nontronite from the Red Sea, by Corliss *et al.* (1978) for a nontronitic clay from hydrothermal mounds near the Galapagos Rift, and by Hoffert *et al.* (1978) for FAMOUS samples from the Atlantic Ocean. Ferrous iron was not detectable by chemical analysis or by Mössbauer spectroscopy. Indeed, ferrous iron has been reported in only one marine hydrothermal nontronite from the Red Sea (Bischoff, 1972). The near-monomineralic nature of the present clay sample is indicated by its very low Ca, Na, P, Mn, and Ti contents. The Mg and K contents are similar to those reported for many hydrothermal nontronites (Table 1).

Based on this chemical composition and assuming a monomineralic character for the material, the following structural formula is proposed for the NH_4-saturated nontronite:

$$(K_{0.30}(NH_4^+)_{0.69}(Fe^{3+}_{3.32}Mg_{0.81})(Si_{7.33}Fe^{3+}_{0.67})O_{20}(OH)_4.$$
$$\text{sum} = 4.13 \qquad \text{sum} = 8.00$$

The amount of tetrahedral iron calculated from the chemical analysis is in complete agreement with that deduced by Mössbauer spectroscopy. XRD data and IR spectra suggest an unequal distribution of the layer charge and octahedral site occupancy of the nontronite. Unequal charge distribution is also suggested by the observation that some of the interlayer K^+ could not be replaced by NH_4^+. Thus, this structural formula merely represents an average composition of the mineral.

The interlayer charge as calculated from the formula is somewhat larger than the charge suggested by the cation-exchange capacity (97 meq/100 g) determined separately (Table 1), and more than half of the charge originates in the tetrahedral sheets. McMurtry *et al.* (1983) assigned no tetrahedral iron to the nontronite from the Galapagos hydrothermal mounds; yet, as the data compiled by Hoffert (1980) show, tetrahedral iron is a characteristic feature of many hydrothermal nontronites (Table 2). The concentrations of octahedral Mg and interlayer K^+ appear to be within the range common for hydrothermal nontronites.

From the basal spacings of untreated bulk nodule material, the exchangeable cations appear to be mostly divalent. From the specific surface area of the clay sample (550 m^2/g) and its CEC, the charge density is 1.76×10^{-10} eq/cm^2 or 5.09×10^{-4} esu/cm^2, similar to the value obtained by Newman (1983) for beidellite from the Black Jack mine in Idaho.

Using the Fe–Mn–(Co + Cu + Ni) ternary diagram proposed by Bonatti *et al.* (1972), Hoffert (1980) showed that most of the minor element compositions of hydrothermal smectites are poor in Mn and transition metals and therefore cluster close to the Fe apex. From Table 1 it can be seen that the KL9 nontronite is particularly low in Cu (not detectable), Ni, Co, and Mn and therefore exemplifies this trend. Zn is higher than the values reported by Corliss *et al.* (1978) for the Galapagos Rift nontronite and by Hoffert *et al.* (1978) for the FAMOUS hydrothermal clays. The Cr content is similar to the values cited by Hoffert *et al.*, but higher than those given for the pure nontronite by Corliss *et al.* (1978). The V content is within the range given for hydrothermal clays. Whereas metalliferous hydrothermal sediments commonly are greatly enriched in Ba, hydrothermal clay minerals are low in Ba, and the Ba content of the KL9 nontronite is even lower than those reported hitherto. Pb is considerably lower than the values cited by Hoffert (1980) for the Galapagos Rift nontronite. No comparable values for Sr and Rb were found in the literature.

NONTRONITE FORMATION

Oxygen isotope analysis of the purified <0.6-μm fraction of KL9 nontronite gave $\delta^{18}O = 26 \pm 0.3‰$ relative to SMOW. Using the geothermometric equation of Yeh and Savin (1977) for smectite–water: $1000_{ln} = 2.67 \cdot 10^6 \cdot T^{-2} - 4.82$, and assuming $\delta^{18}O$ of 0.0 for seawater, a formation temperature of 21.3–22.8°C can be calculated, close to the lowest temperature of formation deduced by McMurtry *et al.* (1983) for Al-poor nontronite formed in Galapagos mounds sediments. The ratio $Fe_2O_3/(MgO + Al_2O_3)$ vs. $\delta^{18}O$ for sample KL9 falls within the field of deep-sea authigenic nontronites delineated by McMurtry *et al.* (1983, Figure 5).

The two features cited by Harder (1976) as critical for the formation of nontronite are relatively low Si concentrations and the presence of reduced iron in solution. Scanning electron micrographs revealed the nearly perfect euhedral habit of quartz crystals embedded in the nontronite clay matrix (Figure 5c). According to Stoffers *et al.* (1984), oxygen isotope data indicate that these crystals were formed at 25°C. Harder

(1971) noted that quartz crystallizes at such low temperatures only from solutions which are undersaturated in SiO_2 with regard to quartz (i.e., <2.8 ppm SiO_2). Because no other less-crystalline silica phases were identified in the KL9 sediment, soluble Si during quartz crystallization must have been in this range.

Because the quartz crystallites were found embedded in the clay matrix, and even coating clay granules, nontronite precipitation must have preceded quartz crystallization. Thus, silica in solution during nontronite formation may have been only slightly oversaturated with respect to quartz, and probably was below the 20 ppm SiO_2 indicated by Harder (1976). Oxygen isotope geothermometry of the authigenic quartz and nontronite showed that both minerals were formed under closely similar thermal regimes.

Oxidation gradients in core KL9 are indicated by the vertical Fe-Mn segregation, which is governed by the balance between oxygen-poor hydrothermal fluids at the bottom and oxygen-rich seawater diffusing downward. In the presence of the hydrothermal fluids Mn was brought into solution while nontronite precipitated. Mn precipitated higher up in the sediment where the redox potential was higher. A similar process has been proposed for the formation of the nontronites in the Galapagos sediment mounds by Dymond *et al.* (1980). Coating of nontronite granules by Mn oxides possibly indicates fluctuations in the oxidation gradient.

The KL9 nontronite contains significant amounts of interlayer K^+, like many other hydrothermal nontronites; it may therefore represent a transition stage in the "celadonitization" process of the smectite by adsorption of K from seawater, as suggested by Rateev *et al.* (1980).

The $^{87}Sr/^{86}Sr$ ratio obtained for sample KL9 was 0.71157 ± 0.0002, considerably larger than the value of 0.70907 characteristic of modern seawater (Burke *et al.,* 1982). As both increasing age of seawater and basalt-seawater interaction cause a decrease in the Sr isotope ratio, some of the ^{87}Sr must be radiogenic. On the basis of the observed Rb/Sr ratio, and using the appropriate Sr isotope ratio of seawater of that age, a minimum time of formation of the nontronite of 12 million years can be deduced. Any contribution of basalt Sr, like that observed in other authigenic deep-sea smectites (Staudigel *et al.,* 1981) would increase the calculated age of formation of the nontronite. The area from which the sample was collected was dated at 25 million years by geomagnetic polarity (Plate Tectonic Map, 1981). If the nontronite formed at that time, the initial $^{87}Sr/^{86}Sr$ ratio would have been about 0.706, a value that could have been attained by seawater-basalt interaction.

The uncertainties involved in a single isotope analysis preclude definitive dating of the sample. It can, however, be established that the nontronite was formed at least 12 million years ago and may even be as old as the area in which is was found (25 million years), having been formed *in situ* in the vicinity of the active ridge.

ACKNOWLEDGMENTS

The support given by the Deutsche Forschungsgemeinschaft (DFG) to the author from the Federal Republic of Germany is gratefully acknowledged. Thanks are also due to Prof. R. Bauminger of the Department of Physics and to Dr. A. Matthews of the Department of Geology of the Hebrew University for the Mössbauer spectra and the oxygen isotope determinations, respectively. We also thank Dr. G. McMurtry for his constructive criticism.

REFERENCES

Bischoff, J. L. (1972) A ferroan nontronite from the Red Sea geothermal system: *Clays & Clay Minerals* **20,** 217–223.

Bonatti, E., Kraemer, T., and Rydell, H. S. (1972) Classification and genesis of submarine iron-manganese deposits: in *Ferro-manganese Deposits on the Ocean Floor,* D. R. Horn, ed., Arden House, New York, 149–166.

Brigatti, M. F. (1983) Relationships between composition and structure in Fe-rich smectites: *Clay Miner.* **18,** 177–186.

Burke, W. H., Denison, R. E., Hetherington, E. A., Koepnick, R. B., Nelson, H. F., and Otto, J. B. (1982) Variation of seawater $^{87}Sr/^{86}Sr$ throughout Phanerozoic time: *Geology* **10,** 516–519.

Carter, D. L., Heilman, M. D., and Gonzalez, C. L. (1965) Ethylene glycol monoethyl ether for determining surface area of silicate minerals: *Soil Sci.* **100,** 356–360.

Čičel, B. and Machajdik, D. (1981) Potassium and ammonium-treated montmorillonites. I. Interstratified structures with EG and water: *Clays & Clay Minerals* **29,** 40–46.

Cole, T. G. and Shaw, H. F. (1983) The nature and origin of authigenic smectites in some recent marine sediments: *Clay Miner.* **18,** 239–252.

Corliss, J. B., Lyle, M., Dymond, J., and Crane, K. (1978) The chemistry of hydrothermal mounds near the Galapagos Rift: *Earth Planet. Sci. Lett.* **40,** 12–24.

Despraires, A. (1983) Relation entre le parametre *b* des smectites et leur contenu en fer et magnésium. Application à l'étude des sédiments: *Clay Miner.* **18,** 165–175.

Dymond, J., Corliss, J. B., Cobler, R., Murati, Ch. M., Chou, C., and Conard, R. (1980) Composition and origin of sediments recovered by deep drilling of sediment mounds, Galapagos Spreading Center: in *Initial Reports of Deep-Sea Drilling Project, Vol. 54,* B. R. Rosendahl, R. Hekinian *et al.,* eds., U.S. Government Printing Office, Washington, D.C., 377–385.

Eggleton, R. A. (1977) Nontronite: chemistry and X-ray diffraction: *Clay Miner.* **12,** 181–194.

Goodman, B. A., Russell, J. D., Fraser, A. R., and Woodham, F. W. D. (1976) A Mössbauer and IR spectroscopic study of the structure of nontronite: *Clays & Clay Minerals* **24,** 53–59.

Grimm, R. E. and Güven, N. (1978) *Bentonites:* Elsevier, Amsterdam, 256 pp.

Harder, H. (1971) Quartz and clay mineral formation at surface temperatures: *Mineral. Soc. Japan Spec. Rep.* **1,** 106–108.

Harder, H. (1976) Nontronite synthesis at low temperatures: *Chem. Geol.* **18,** 169–180.

Hoffert, M. (1980) Les "argiles rouges des grands fonds" dans le Pacifique Centre Est: authigenèse, transport, diagenèse: *Sci. Geol. Strasbourg* **61,** 231 pp.

Hoffert, M., Perseil, A., Hekinian, R., Choukroune, P., Needham, H. D., Francheteau, J., and Le Pichon, X. (1978) Hydrothermal deposits sampled by diving saucer in Transform Fault "A" near 37°N on the Mid-Atlantic Ridge. Famous Area: *Oceanologica Acta* **1,** 73–86.

Kurnosov, V., Kholodkevich, I., Kokorina, L., Kotov, N., and Chudaev, O. (1982) The origin of clay minerals in the oceanic crust revealed by natural and experimental data: in *Proc. Inter. Clay Conf., Bologna, Pavia 1981,* H. van Olphen and F. Veniale, eds., Elsevier, Amsterdam, 547–556.

MacEwan, D. M. (1961) Montmorillonite minerals: in *The X-ray Identification and Crystal Structures of Clay Minerals,* G. Brown, ed., Mineralogical Society, London, 143–207.

McMurtry, G. M., Wang, Chung-Ho, and Yeh, Hsueh-Wen (1983) Chemical and isotopic investigations into the origin of clay minerals from the Galapagos Hydrothermal Mound Field: *Geochim. Cosmochim. Acta* **47,** 475–489.

Méring, J. and Oberlin, A. (1971) The smectites: in *The Electron-Optical Investigation of Clays,* J. A. Gard, ed., Mineralogical Society, London, 193–230.

Moorby, S. and Cronaw, D. (1983) The geochemistry of hydrothermal and pelagic sediments from the Galapagos Hydrothermal Mounds Field, DSDP Leg 70: *Mineral. Mag.* **47,** 291–300.

Newman, A. C. (1983) The specific surface of soils determined by water absorption: *J. Soil Sci.* **34,** 23–32.

Plate Tectonic Map (1981) Plate Tectonic Map of the Circum-Pacific Region, SE Quadrant: Amer. Assoc. Petrol. Geol., Tulsa, Oklahoma.

Rateev, M. A., Timofeev, P. P., and Rengarten, N. V. (1980) Minerals of the clay fraction of Pliocene Quaternary sediments of the East Equatorial Pacific: in *Initial Reports of the Deep-Sea Drilling Project, Vol. 54,* B. R. Rosendahl, R. Hekinian *et al.,* eds., U.S. Government Printing Office, Washington, D.C., 307–318.

Rozenson, I., Bauminger, E. R., and Heller-Kallai, L. (1979) Mössbauer spectroscopy of iron in 1:1 phyllosilicates: *Amer. Miner.* **64,** 893–901.

Schrader, E. L., Rosendahl, B. R., Furbish, W. J., and Mattey, D. P. (1980) Mineral and geochemistry of hydrothermal and pelagic sediments from the mounds hydrothermal fields, Galapagos Spreading Center: DSDP, leg 54: *J. Sediment. Petrol.* **50,** 917–927.

Staudigel, H., Hart, S. R., and Richardson, S. H. (1981) Alteration of the oceanic crust: processes and timing: *Earth & Planet. Sci. Lett.* **52,** 311–327.

Stoffers, P., Pluger, W., Lallier-Verges, E., Schmitz, W., and Hoffert, H. (1984) A new hydrothermal deposit in the South Pacific: *Mar. Geol.* (in press.)

Sudo, T., Shimoda, S., Yotsumoto, H., and Aita, S. (1981) *Electron Micrographs of Clay Minerals:* Elsevier Sci. Publ., Amsterdam, 203 pp.

Weaver, C. A. and Pollard, L. D. (1973) *The Chemistry of Clay Minerals:* Elsevier, Amsterdam, 213 pp.

Yeh, H. W. and Savin, S. M. (1977) Mechanisms of burial metamorphism of argillaceous sediments. 3. O-isotope evidence: *Geol. Soc. Amer. Bull.* **88,** 1321–1330.

(Received 31 August 1983; accepted 7 April 1984)

Резюме—Смектит, близкий чистому Fe конечному члену серии нонтронит-бейделлит, обнаруживался в мелкой глине, отделенной из 354 цм глубокой колонки осадка в юго-западном районе Тихого Океана. Минерал имеет ось *b* равную 9,09 Å и необыкновенно низкую температуру дегидроксилирования и состоит из связок волокон менее, чем 50 Å широких. Плотность заряда равна 5,09 × 10^{-4} эсе/цм². Заряд возникает, главным образом, в следствие присутствия 18% всех атомов Fe в тетраэдрических местах, как это было определено при помощи анализа Мессбауера. Небольшие отклонения инфракрасного спектра этого минерала от спектра нонронита являются результатом присутствия большого количества октаэдрического Mg. Присутствие аутигенного вкарца в этом же самом образце дает возможность какого-либо предположения концентрации растворенного кремния во время генезиса нонтронита. Значение $\delta^{18}O$, равное 26 ± 0,3‰, указывает на температуру формирования около 22°C. Sr изотопный состав показывает, что нонтронит образовался по крайней мере 12 миллионов лет тому назад. [E.G.]

Resümee—Ein Smektit, der in der Zusammensetzung dem reinen Fe-Endglied der Nontronit-Beidellit-Mischungsreihe sehr nahekommt, wurde in der feinen Tonfraktion, die von einem 354 cm tiefen Sedimentbohrkern von südwestlichen Pazifik Becken abgetrennt wurde, gefunden. Das Mineral hat eine kleine *b*-Achse von 9,09 Å und eine ungewöhnlich niedrige Dehydroxilierungstemperatur von 454°C und ist aus Faserbündeln zusammengesetzt, die eine Dicke unter 50 Å haben. Seine Ladungsdichte beträgt 5,09 × 10^{-4} esu/cm². Die Ladung rührt hauptsächlich von der Anwesenheit von 18% Gesamteisen in tetraedrischer Koordination her, wie aus der Mössbauerbestimmung hervorgeht. Geringe Abweichungen der Infrarotspektren von denen, die für Nontronit angegeben werden, kommen wahrscheinlich durch die Anwesenheit von mehr oktaedrischem Mg. Die Anwesenheit von autigenem Quarz in der gleichen Probe erlaubt einige Spekulationen über die Konzentration des gelösten Siliziums während der Nontronitentstehung. Ein $\delta^{18}O$-Wert von 26 ± 0,3‰ deutet auf eine Bildungstemperatur von etwa 22°C hin. Das Sr-isotopenverhältnis läßt darauf schließen, daß der Nontronit vor mindestens 12 Millionen Jahren gebildet wurde. [U.W.]

Résumé—De la smectite proche du membre terminal Fe pur de la série nontronite-beidellite a été trouvée dans l'argile fine séparée d'une carotte sédimentaire de 354 cm de profondeur dans la Basin Pacifique du sud-ouest. Le minéral a un axe-*b* de 9,09 Å et une température de déshydroxylation inhabituellement basse de 454°C et est composé d'un ensemble de fibres d'une longueur de moins de 50 Å. Sa densité de charge est $5{,}09 \times 10^{-4}$ esu/cm^2. L'origine de la charge est principalement due à la présence de 18% du Fe total en positions tétraèdrales, comme l'a déterminé l'analyse de Mössbauer. De légères déviations des spectres infrarouges par rapport à ceux déterminés pour des nontronites sont probablement dues à la présence de plus de Mg octaèdral. La présence de quartz authigénique dans le même échantillon permet quelque speculation quant à la concentration de silice dissoute pendant la genèse nontronite. Une valeur $\delta^{18}O$ de $26 \pm 0{,}3‰$ indique une température de formation d'environ 22°C. La proportion d'isotope Sr suggère que la nontronite s'est formée il y a au moins 12 million d'années. [D.J.]

https://doi.org/10.1346/CCMN.1984.0320505 Published online by Cambridge University Press